NASA Technical Memorandum 82823

Factors Influencing the Thermally-Induced Strength Degradation of B/Al Composites

James A. DiCarlo
Lewis Research Center
Cleveland, Ohio

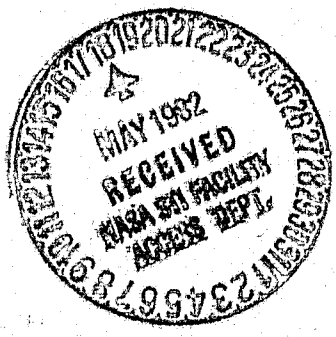

Prepared for the
Symposium on Failure Modes in Metal Matrix Composites
sponsored by the American Institute of Mining, Metallurgical and Petroleum Engineers
Dallas, Texas, February 15-18, 1982

NASA

FACTORS INFLUENCING THE THERMALLY-INDUCED STRENGTH DEGRADATION OF B/Al COMPOSITES*

by James A. DiCarlo

E-1175

Abstract

Literature data related to the thermally-induced strength degradation of B/Al composites were examined in the light of fracture theories based on reaction-controlled fiber weakening. Under the assumption of a parabolic time-dependent growth for the interfacial reaction product, a Griffth-type fracture model was found to yield simple equations whose predictions were in good agreement with data for boron fiber average tensile strength and for unidirectional B/Al axial fracture strain. The only variables in these equations were the time and temperature of the thermal exposure and an empirical factor related to fiber surface preparation prior to aluminum reaction. Such variables as fiber diameter and aluminum alloy composition were found to have little influence. The basic and practical implications of the fracture model equations are discussed.

* Technical paper to be presented at the Symposium on Failure Modes in Metal Matrix Composites sponsored by the Metallurgical Society of AIME, Dallas, Texas, February 15-18, 1982.

Key Words: Boron/Aluminum Composite, Thermal Exposure, Boron Fiber Strength, Composite Fracture Strain, Reaction-Controlled Fracture, and Chemical Polish.

FACTORS INFLUENCING THE THERMALLY-INDUCED STRENGTH DEGRADATION OF B/Al COMPOSITES*

by James A. DiCarlo
National Aeronautics and Space Administration
Lewis Research Center
Cleveland, Ohio 44135

Introduction

At the high temperatures typically employed for the fabrication of boron/aluminum (B/Al) composites, boron fibers react with the aluminum matrix, forming a weak interfacial reaction product whose growth eventually leads to a loss in fiber and composite strength (1,2). To avoid or minimize this strength degradation problem, it would be of great value to develop a basic understanding of the nature and quantitative contribution of the significant physical factors which influence reaction product formation and its eventual control of fiber fracture. The objective of this paper is to gain such an understanding by carefully examining literature data related to B/Al strength degradation and then analyzing these data in the light of appropriate physical theories concerning interface formation and interface-induced fiber fracture. The results of this study will show that the fracture characteristics of thermally-exposed B/Al composites can be explained well by Griffth fracture theory and the parabolic time-dependent growth of a cracked interfacial reaction product. They will also show that thermally-induced degradation in fiber and composite fracture properties can be empirically described by simple equations involving exposure time and temperature. Aluminum alloy composition and fiber diameter were found to negligibly influence reaction-controlled fracture. However, chemical polishing of the fiber surface prior to aluminum reaction can have a significant beneficial effect.

Discussion

To illustrate typical aluminum reaction effects on boron fiber fracture, the first part of this Discussion section will examine some recent data concerning the thermally-induced strength degradation of aluminum-coated boron fibers. The second part will then present and discuss the assumptions of two theoretical fiber fracture models which have been proposed in the literature to explain the physical influence of the boron-aluminum reaction product on fiber strength. In the third part, the validity of the fracture models will be investigated by comparing their predictions with experimental data concerning the time-temperature dependent fracture of thermally-exposed B/Al composites. Finally, the last part of the Discussion will analyze data which show that chemically polishing boron fibers before subjecting them to aluminum reaction can significantly minimize strength degradation effects.

1. Strength Degradation of Al-Coated Fibers

In order to obtain a fundamental understanding of fiber-matrix reaction effects in B/Al composites, DiCarlo and Smith (3) recently measured the room temperature tensile and flexure strengths of aluminum-coated 203 μm diameter boron fibers which were isothermally exposed for one hour at temperatures

typically employed for B/Al fabrication. The pure aluminum coatings were applied at low temperature by ion-plating techniques. Because the coating thicknesses were in the range 2 to 4 μm, their load bearing contributions to the fiber fracture stress could be neglected. The results for $\bar{\sigma}_f$ (25 mm), the average fiber tensile strength at a 25 mm gauge length, are plotted as a function of exposure temperature in the lower curve of Fig. 1. These data show that the fibers retained their original as-produced strengths to 470° C at which point the effects of the boron-aluminum interfacial reaction product began to degrade fiber strength. Thus, as temperature increased above 470° C, the average stress required to initiate fiber fracture from reaction-induced flaws decreased to a level below that required for fracture from strength-limiting flaws in the as-produced fibers. Microscopic fracture surface studies revealed that the reaction-induced flaws were located on the fiber surface whereas strength-limiting flaws for the as-produced fibers were located either on the fiber surface or within the fiber's tungsten-boride core.

Because the fiber and composite fracture theories discussed in the next section require knowledge of the Weibull modulus for reaction-controlled fracture, it is of interest here to also examine the average flexure strength results for the aluminum-coated fibers. These data which are plotted in the upper curve of Fig. 1 show a similar threshold temperature for degradation as the tensile data, but are about a factor of 1.6 larger in magnitude than the tensile data. Since reaction flaws were located only on the fiber surface, DiCarlo and Smith (3) were able to use Weibull statistical theory (4) to show that the higher flexure strengths were due to the fact that the effective gauge length for the flexure test was ~ 2.5 mm as compared to 25 mm for the tensile test. That is, Weibull theory predicts that the average fiber strength $\bar{\sigma}_f$ should increase with decreasing gauge length L according to:

$$\bar{\sigma}_f(L_1)/\bar{\sigma}_f(L_2) = (L_2/L_1)^{1/\omega} \qquad (1)$$

where ω is the Weibull modulus. Thus, from the Fig. 1 data, one obtains $1.6 \simeq (10)^{1/\omega}$ so that the Weibull modulus characterizing reaction-controlled fracture is ~ 5. This ω value is consistent with the scatter in the strength results observed at constant gauge length. For example, strength coefficients of variation from 15 to 20 percent were measured which imply (4) Weibull moduli ranging from 6 to 8.

2. Reaction-Controlled Fracture Theory

The two primary fracture models that have been proposed to explain aluminum reaction effects on boron fiber fracture assume that the strength decrease with increasing temperature is associated with the growth in thickness of a strength-controlling interfacial reaction product on the fiber surface. Model I proposed by Metcalfe and Klein (1) assumes that due to growth defects within its structure, the reaction product cracks across its thickness, h, at a strain lower than that of the unreacted fiber. Because of good bonding to the fiber surface, the cracked reaction product becomes a surface crack of length h and therefore controls average fiber strength according to Griffth theory; that is:

$$\bar{\sigma}_f = \sigma_f^u(L) \qquad \text{for} \quad \sigma_f^u \leq \sigma_f^r \tag{2a}$$

and

$$\bar{\sigma}_f = \sigma_f^r(L) = B/[\bar{h}(L)]^{1/2} \qquad \text{for} \quad \sigma_f^u > \sigma_f^r. \tag{2b}$$

Here σ_f^u and σ_f^r are the average fiber strengths controlled by as-produced flaws and interfacial cracks, respectively; B is a material constant; and $\bar{h}(L)$ is the average crack size controlling σ_f^r for a test gauge length L. The gauge length dependence was introduced into the thickness h to account for the Fig. 1 results which show that after the same thermal degradation treatment, $\bar{\sigma}_f$ decreased with increasing gauge length, implying by Eq. (2b) that the average size $\bar{h}$ of the strength-limiting cracks was increasing with gauge length. Thus, according to Model I, the distribution in fiber strength is explained by a distribution in reaction product thickness.

Model II, a fracture model proposed by Shorshorov et al. (5), assumes that fiber fracture occurs simultaneously with reaction product fracture because the local stress at the newly formed crack tip is greater than the fiber cohesive strength which is assumed equal to 10 percent of the fiber elastic modulus. These authors also assume that the average strength of the interfacial reaction product $\bar{\sigma}_i$ is controlled by Weibull statistics; that is:

$$\bar{\sigma}_i(V_1) = \bar{\sigma}_i(V_2)[V_2/V_1]^{1/\beta}. \tag{3}$$

Here V is the reaction product volume and β is the Weibull modulus characterizing the product strength distribution. Presumably β is related to the size and spatial distribution of growth flaws within the reaction product. Thus, according to Model II, average fiber strength under reaction conditions should obey the relation

$$\bar{\sigma}_f = \frac{E_f}{E_i}\bar{\sigma}_i(V_1) = \frac{E_f}{E_i}\bar{\sigma}_i(V_2)\left[\frac{L_2}{L_1}\right]^{1/\beta}\left[\frac{D_2}{D_1}\right]^{1/\beta}\left[\frac{h_2}{h_1}\right]^{1/\beta}. \tag{4}$$

Here E_f and E_i are the elastic moduli of the fiber and interface layer, respectively; and the interface volume V has been replaced by the product of the test gauge length L, the fiber diameter D, and the interface thickness h. It follows then that under this model, if D is constant and h is position-independent, any observed gauge length dependence for average fiber strength can be used to measure the Weibull modulus β. Assuming this to be the case for the Fig. 1 results, these data yield $\beta = \omega \approx 5$. On the other hand, if h does depend on position as, for example, $(h_2/h_1) = (L_2/L_1)^{1/\eta}$, Eq. (4) and Fig. 1 yield $\beta = \omega(1+1/\eta)$ so that $\beta > 5$ for $\eta > 0$. Thus, if Model II is applicable for the boron-aluminum reaction, Eq. (4) with $\beta \geq 5$ should predict fiber strength degradation as h increases.

To put the fracture model equations into forms suitable for direct comparison with time and temperature dependent fracture data, consideration should be given to the physical mechanisms and kinetics influencing the growth of the interface thickness h. Microscopic studies using thermally-exposed B/Al composites have observed that the boron-aluminum reaction product consists of acicular or needle-type crystals emaninating from the fiber surface (1,2). The shape and structure of these crystals were found to depend on alloying constituents in the aluminum matrix (6). Obviously this type of growth pattern is far from the uniform interface structure implicit in the assumptions of Model I and II. Nevertheless, for the purpose of determining the general applicability of these models, one might as a crude approximation assume that crystal height above the fiber surface is equivalent to interface thickness h. Then, because the growth kinetics of boron-containing interfacial reaction products are typically characterized by a diffusion-limited parabolic time dependence (7,8), one might also assume that the crystal height for the boron-aluminum reaction product increases with time and temperature according to:

$$h = \alpha t^{1/2} \exp[-Q/2kt]. \tag{5}$$

Here α is a normalizing constant, t is exposure time, T is exposure temperature in Kelvin, k is Boltzman's constant, and Q is the activation energy controlling product growth. Since crystal shape is observed to be matrix dependent, the parameters α and Q may depend on alloying constituents in the aluminum.

Support for the parabolic time-dependent growth for the boron-aluminum reaction product can be obtained from scanning electron micrographs of Klein and Metcalfe (2) who studied B/6061-Al composites that were exposed for various times at 504° C. Using the micrographs to measure maximum crystal height and plotting these heights as a function of $(t)^{1/2}$, one obtains the results shown in Fig. 2. Although the scatter is large, the data clearly support a linear relationship between h and $t^{1/2}$.

Assuming the parabolic growth Eq. (5) and the fracture model Eqs. (2b) and (4), one then obtains the general result that under reaction-controlled conditions, average fiber strength should depend on time and temperature according to:

$$\bar{\sigma}_f(L) = Ct^{-1/2m} \exp[U/T] \tag{6}$$

where C is an empirically determined constant. For Model I, $C = C(L)$, $m = 2$, and $U = Q/4k$. For Model II, $C = C(L,D)$, $m = \beta \geq 5$, and $U = Q/2\beta k$.

The degradation in average fiber strength predicted by Eq. (6) can also be used to predict the time and temperature dependent degradation in fracture strain of a unidirectional B/Al composite. Unlike composite tensile strength which contains both a fiber and matrix contribution, composite axial fracture strain ε_c is, to a good approximation, independent of matrix behavior. For this reason, it is possible to directly relate ε_c to the $\bar{\sigma}_f(L)$ for the reinforcing fibers. In fact, if composite fracture occurs by the cumulative fracture of individual fibers (9), the Appendix shows that:

$$\varepsilon_c E_f = \sigma_{bf} = G\bar{\sigma}_f(L). \tag{7}$$

Here σ_{bf} is the effective fiber bundle strength within the composite and G is a constant which is independent of reaction conditions. Thus, according to Eqs. (6) and (7), the two fiber fracture models predict that

$$\varepsilon_c = \varepsilon_c^u \qquad \text{for} \quad \varepsilon_c^u \leq \varepsilon_c^r$$

and (8)

$$\varepsilon_c = \varepsilon_c^r = Ht^{-1/2m} \exp[U/T] \qquad \text{for} \quad \varepsilon_c^u > \varepsilon_c^r .$$

Here ε_c^u is the composite fracture strain under conditions in which the fibers maintain their as-produced strengths, ε_c^r is composite fracture strain under reaction-controlled conditions, and $H = CG/E_f$ is a normalizing empirical constant. As discussed in the Appendix, axial fracture strain and thus the H parameter should be independent of composite gauge length for test sections longer than the ineffective length (9) which is typically in the range 2 to 8 mm for B/Al composites.

3. Time and Temperature-Dependent Fracture

Having established theoretical equations for thermally-induced fiber and composite strength degradation, let us now examine their validity by comparring their predictions with time and temperature-dependent fracture data.

Turning first to multifilament composite fracture, the time-dependent axial fracture strain data of Klein and Metcalfe (2) are plotted in Fig. 3 for B/Al composites which were isothermally exposed at 538° C. The composites consisted of a 6061 aluminum alloy matrix reinforced by 48 volume percent of 142 μm diameter fibers. Best fitting Eq. (8) to these data, one obtains the solid and dashed curves in Fig. 3 for fracture Models I and II, respectively. Clearly the $m \geq 5$ values for Model II do not fit the data, indicating that the assumptions of Model II are probably not valid for the boron-aluminum reaction product. On the other hand, the good empirical fit of Eq. (8) using $m = 2$ supports the assumptions involved in Model I fracture, parabolic growth, and cumulative weakening. The Fig. 3 result showing deviation from $m = 2$ behavior at strains below 0.3 percent appears to be related to a change in composite fracture mode since the average fracture strain of fibers extracted from highly degraded composites can fall well below 0.3 percent (10). This implies that Eq. (8) for ε_c degradation should only be compared with ε_c data greater than 0.3 percent whereas Eq. (6) for $\bar{\sigma}_f$ has no such restriction.

To verify whether Eqs. (6) and (8) using Model I parameters could also predict reaction-controlled fracture at other temperatures, the logarithms of fiber strength data were plotted in Fig. 4 as a function of the reciprocal absolute temperature at which the fibers were heat treated. For this plot, two types of strength data were obtained from the literature. The first type were average strengths measured at 25 mm gauge length both for aluminum-coated fibers and for fibers which were extracted from heat-treated

multifilament B/Al composites. These $\bar{\sigma}_f$ (25 mm) data are plotted as open points. The second type were fiber bundle strengths as calculated from $\sigma_{bf} = E_f \varepsilon_c$ where the ε_c are axial fracture strain data for multifilament B/Al composites and E_f is the fiber modulus taken as 400 GN/m^2. Only those experimental results were used in which ε_c data were directly measured or could be easily calculated from fracture stress data and published stress-strain curves. The σ_{bf} data are plotted as closed points. To account for differences in exposure time t (hours), all strength data were normalized to a one-hour exposure by multiplying the experimental data by $(t)^{1/4}$. That is, it was assumed that the time dependence obeyed parabolic growth and the Model I fracture assumptions.

Examination of Fig. 4 shows that over a large temperature range, all reaction-controlled strength data can be fit well to the same straight line. The implications of this result are many. First, it indicates that with $C = 3.5 \times 10^{-4}$ GN/m^2, $H = 8.8 \times 10^{-7}$, $m = 2$, and $U = 7060$ K, Eqs. (6) and (9) can be used to give good estimates of reaction effects on average fiber tensile strength and on the axial fracture strain of unidirectional B/Al composites. Second, it shows that under reaction-controlled conditions, $G = 1$ so that little difference exists between average fiber strength measured at 25 mm gauge length and effective fiber bundle strength in B/Al composites. Third, it indicates that at least empirically, fiber diameter and matrix alloy composition (1100 or 6061) have little effect on fiber fracture as described by Eq. (8). The apparent absence of a diameter dependence is another fact in opposition to Model II fracture theory (cf. Eq. (4)). Fourth, the assumptions of Model I fracture, parabolic interfacial growth , and cumulative weakening for B/Al composites appear to conform to reality. Finally, assuming the validity of these assumptions, the best fit U value suggests that Q, the energy controlling interfacial growth, is $4kU = 2.4$ eV (56 kcal/mole).

It should be mentioned that although the effects of time and temperature on composite fracture strain degradation can now be accounted for by Eq. (8), this simple empirical equation should only apply for conditions involving continuous thermal exposure and should not be accurate for cyclic types of thermal exposure. This is due to the fact that after being thermally cycled between a low and high temperature, the strength of B/Al composites have been observed to degrade to a lower level then the strength of composites which were isothermally exposed for the same equivalent time at the high temperature (11,12). This result has been explained primarily by the cycling-induced breakup of interfacial structure caused by the mechanical fatigue effects associated with the mismatch in fiber and matrix thermal expansion. Thus, under these conditions, the protective nature inherent in the parabolic type of interfacial growth would not completely exist. Accordingly, the time dependence for strength degradation after thermal cycling might be expected to be closer to $t^{-1/2}$ rather than $t^{-1/4}$ where t is equivalent time at the high temperature. An additional problem associated with thermal cycling is a fatigue-induced debonding between the fiber and matrix which can not only lead to reduced stress transfer and a lower composite strength but also to an exposure of the boron fiber surface to detrimental high temperature reaction with oxygen (13).

The strength data plotted in Fig. 4 were all measured at room temperature where the boron fibers deform elastically. However, if B/Al composites are tested at elevated temperatures, the boron fibers creep, resulting in a loss in composite strength entirely different than the reaction-induced strength loss. DiCarlo studied this creep problem (14) and concluded that

under fiber creep conditions, composite axial fracture strain ε_c is to a good approximation independent of the time t' and the temperature T' during which tensile loading is applied. However, composite strength will fall off according to:

$$\sigma_c \cong \overset{\circ}{\sigma_c}/A(t',T') \tag{9}$$

where $\overset{\circ}{\sigma_c}$ is the room temperature composite strength and A (t',T') is a fiber creep function which increases from a value of unity as the time and temperature of loading increase. It follows then that for high temperature applications, B/Al tensile strength could depend both on the time-temperature conditions involved in the exposure and also on the time-temperature conditions involved in the loading. On the other hand, B/Al fracture strain will depend only on exposure conditions. Thus, even if B/Al composites were under axial loading at boron-aluminum reaction temperatures, Eq. (8) with the empirical constants from Fig. 4 should still yield a good estimate of composite fracture strain.

4. Chemical Polishing Effects

In their study of aluminum reaction effects, DiCarlo and Smith (3) also measured the thermally-induced strength degradation of aluminum-coated 203 μm diameter boron fibers which were chemically polished in nitric acid prior to the coating and thermal exposure. The initial polish treatment yielded fibers with higher average strength and lower strength scatter than the original as-produced fibers. The improved strength properties were caused by the removal of low-strength high-variability flaws from the as-produced fiber surface, thereby leaving fiber fracture to be controlled only by higher-strength lower-variability flaws located within the fiber's tungsten-boride core. After coating the polished fibers with aluminum at low temperature, the fiber strength properties were found to be unchanged. However, after one-hour isothermal exposure at temperatures above 500° C, reaction-related strength degradation effects were observed as shown by the Fig. 5 results for average tensile and flexure strength. These data were measured at room temperature using coated pre-polished fibers with reduced diameters of 195, 180, and 140 μm.

Comparing the two data sets of Fig. 5 with the corresponding data sets of Fig. 1, one observes that for the same test and reaction conditions, the average strength of the coated pre-polished fibers was on the average a factor of 1.6 greater than that of the coated as-produced fibers. In addition, the threshold temperature for tensile strength degradation was ~ 45° C higher for the pre-polished fibers. Thus, chemical polishing not only improved the strength properties of unreacted fibers, but also significantly increased the stress levels required for reaction-controlled fracture. This in turn shifted the strength degradation curve for pre-polished fibers to higher temperatures. The practical implications of these results for producing stronger B/Al composites at higher fabrication temperatures are discussed in some detail by DiCarlo and Smith (3).

Any fracture model proposed to explain the beneficial effects of chemical polishing must account for the fact that only slight polishing is required to improve the strengths of both unreacted and reacted fibers. Wawner (15) has suggested that the strength improvement for unreacted fibers

is due to the smoothing of the crack-like structure associated with growth nodules generally found on the surface of as-produced fibers. Because little change in nodule height was observed with slight polishing, DiCarlo and Smith (3) suggest that for unreacted fibers, the primary strengthening effect of polishing is to significantly increase the average radius of curvature r_o at the nodule boundary. This crack blunting concept together with the interfacial fracture mechanism of Model I suggests that under reaction conditions, the lower strengths of the as-produced fibers are controlled by interfacial cracks which terminate at nodule boundaries with an average tip radius r_o, whereas the higher strengths of the pre-polished fibers are controlled by interfacial cracks which terminate randomly on the fiber surface with a larger average tip radius r_i. Presumably r_o is dependent on the as-produced fiber surface structure, whereas r_i is dependent on mechanical properties of the interface alone. Assuming that fibers heat-treated and tested in the same manner have the same interfacial crack depth, it follows then from simple fracture theory (16) that the pre-polished fiber strength should be larger than the as-produced fiber strength by the factor $\varphi = (r_i/r_o)^{1/2}$. For the range of reaction and test conditions examined, the results of Figs. 1 and 5 yield $\varphi = 1.6$. Thus according to this model, sharp nodule boundaries not only act as detrimental flaws for unreacted fibers but also act as stress raisers on interfacial cracks.

Summarizing the polishing results of Fig. 5 and the time-temperature results of Fig. 4, one can now express the thermally-induced strength degradation of boron fibers in contact with aluminum by two simple empirical equations for average fiber tensile strength $\overline{\sigma}_f$ (25 mm) and for composite axial fracture strain ε_c. These equations are

$$\overline{\sigma}_f(25\ \text{mm}) = E_f \varepsilon_c \tag{10}$$

and

$$\varepsilon_c = (8.8\text{x}10^{-7})\varphi t^{1/4} \exp[7060/T]. \tag{11}$$

Here t is exposure time in hours, T is exposure temperature in Kelvin, E_f is 400 GN/m^2, $\varphi = 1$ for as-produced fibers, and $\varphi = 1.6$ for chemically polished fibers. The data of Figs. 3 and 4 indicate that Eqs. (10) and (11) should be accurate to within ±10 percent as long as $\sigma_f < \sigma_f^u$ and 0.3 percent $< \varepsilon_c < \varepsilon_c^u$ where σ_f^u and ε_c^u are the average strength and composite fracture strain for the as-produced unreacted fibers. The excellent predictive accuracy of Eq. (10) for chemically polished fibers is shown by the solid line through the $\overline{\sigma}_f$ (25 mm) data of Fig. 5.

Concluding Remarks

This study has shown that the thermally-induced strength degradation of B/Al composites can be explained well by a fiber fracture model based on the parabolic time-dependent growth of a cracked interfacial reaction product. Simple analytical equations were derived whose predictions were found to be

in good agreement with literature data for the average tensile strength of reacted boron fibers and for the axial fracture strain of isothermally-exposed unidirectional B/Al composites. The only variables in these equations were the time and temperature of the thermal exposure and an empirical factor related to fiber surface preparation prior to composite consolidation. Such factors as fiber diameter and aluminum alloy composition were found to have little influence on reaction-controlled boron fiber fracture.

With the development of the fiber and composite fracture equations, it should now be possible to obtain good estimates of reaction effects for B/Al composites which are subjected to continuous high temperature exposure either during composite fabrication or during structural application. Whereas the composite strain equation could be used to evaluate thermally-induced losses in the axial fracture properties of unidirectional composites, the fiber strength equation could be used to understand general reaction-related fiber weakening for either unidirectional or angle-plied composites. An additional advantage of the fiber strength equation is that it should allow a better understanding of those temperature, time, and fiber surface conditions which must be avoided if the strength properties of the original as-produced fibers are to be retained after composite fabrication.

Appendix

Composite Fracture Theory

Characterizing strength by two-parameter Weibull theory (4), the average tensile strength $\bar{\sigma}_f$ for a group of fibers tested individually at gauge length L is given by:

$$\bar{\sigma}_f = \gamma L^{-1/\omega} \Gamma(1 + 1/\omega) \tag{A1}$$

where γ is a scale parameter, ω is the Weibull modulus, and Γ is the gamma function. If these same fibers are tested as a parallel bundle, the fiber bundle strength is given by:

$$\sigma_{bf} = \gamma L^{-1/\omega} (\omega e)^{1/\omega}. \tag{A2}$$

If the fiber bundle is infiltrated with matrix material to form a unidirectional composite, the fiber bundle strength is generally observed to be greater than that measured without the matrix material. This can be attributed to the fact that the matrix localizes the loss of load carrying ability in a broken fiber, thereby allowing a greater number of individual fibers breaks to occur before complete bundle fracture. Rosen (9) analyzed this cumulative mode of composite weakening and concluded that for a large number of fibers, the fiber bundle strength can be predicted by Eq. (A2) with L replaced by the "ineffective" length δ. For a ductile matrix like aluminum, δ can be estimated from:

$$\delta = \sigma D/2 \tau_{ym} \tag{A3}$$

where $\sigma = \sigma_{bf}$, D is fiber diameter, and τ_{ym} is the shear yield strength of the matrix. An important consequence of Rosen's theory is that the fiber bundle length for a composite is determined by material properties, so that as long as the composite test length L_c is greater than δ, the fiber bundle strength σ_{bf} should be independent of L_c.

Assuming cumulative weakening and neglecting any residual stresses on the fiber, it follows from Eq. (A2) that the axial fracture strain ε_c of a unidirectional composite is given by:

$$\varepsilon_c = \sigma_{bf}(\delta)/E_f = \gamma\delta^{-1/\omega}(\omega e)^{-1/\omega}/E_f \tag{A4}$$

where E_f is fiber modulus. Alternatively, using Eq. (A1) to eliminate γ,

$$\varepsilon_c = \bar{\sigma}_f(L)G/E_f \tag{A5}$$

where

$$G = (L/\delta)^{1/\omega}[(\omega e)^{-1/\omega}/\Gamma(1 + 1/\omega)]. \tag{A6}$$

Thus for composite test lengths greater than δ and reaction conditions characterized by constant ω, composite axial fracture strain should be directly proportional to the average tensile strength of individual reacted fibers extracted from the composites. The proportionality constant G is, however, weakly dependent on fiber diameter through the δ parameter (cf. Eq. (A3)).

References

1. A. G. Metcalfe and M. J. Klein: Interfaces in Metal Matrix Composites, Vol. 1, Composite Materials, A. G. Metcalfe, ed., p. 125, Academic Press, New York, 1974.

2. M. J. Klein and A. G. Metcalfe: AFML TR-71-189, 1971.

3. J. A. DiCarlo and R. J. Smith: NASA TM-82806, 1982.

4. H. T. Corten: Modern Composite Materials, L. V. Broutman and R. H. Krock, eds., pp. 27-105, Addison-Wesley, Reading, Mass., 1967.

5. M. KH. Shorshorov, L. M. Ustinov, A. M. Zirlin, V. I. Olefirenko, and L. V. Vinogradov: J. Mater. Science, 1979, vol. 14, pp. 1850-1861.

6. W. Kim, M. J. Koczak, and A. Lawley: in ICCM/2, Second International Conference on Composite Materials, B. Noton, R. Signorelli, K. Street, and L. Phillips, eds., pp. 487-505, The Metallurgical Society of AIME, New York, 1978.

7. J. A. DiCarlo and T. C. Wagner: NASA TM-82599, 1981.

8. J. Thebault, R. Pailler, G. Bontemps-Moley, M. Bourdeau, and R. Naslain: J. Less Com. Metals, 1976, vol. 47, pp. 221-233.

9. B. W. Rosen: AIAA J., 1964, vol. 2, pp. 1985-1991.

10. M. A. Wright and B. D. Intwala: J. Mater. Science, 1973, vol. 8, pp. 957-963.

11. H. H. Grimes, R. A. Lad, and J. E. Maisel: Met. Trans. A., 1977, vol. 8A, pp. 1999-2005.

12. G. C. Olsen and S. S. Tompkins: NASA Technical Paper 1063, 1977.

13. M. K. White and M. A. Wright: ONR #N00014-75-C0352 NR 031-760, 1976.

14. J. A. DiCarlo: J. Comp. Mater., 1980, vol. 14, pp. 297-314.

15. F. E. Wawner, Jr.: Boron, Vol. 2, Preparation, Properties, and Applications, G. K. Gaule, ed., pp. 283-300, Plenum Press, New York, 1965.

16. A. S. Telelman and A. J. McEvily, Jr.: Fracture of Structural Materials, John Wiley, New York, 1967.

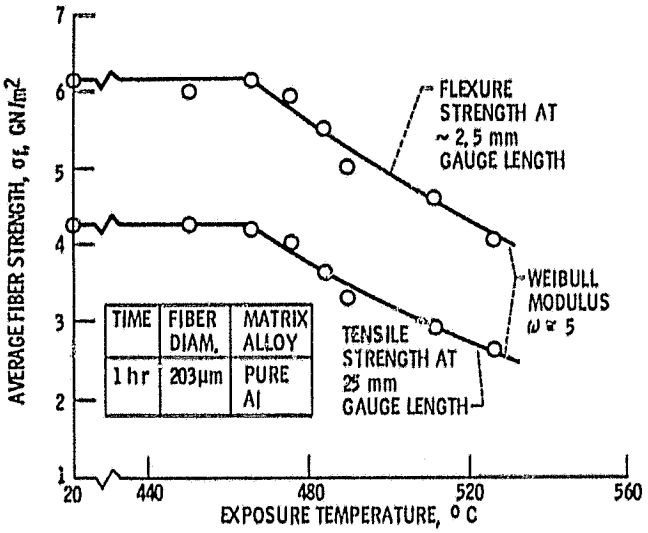

Figure 1. - Tensile and flexure strength degradation for heat-treated aluminum-coated boron fibers (ref. 3).

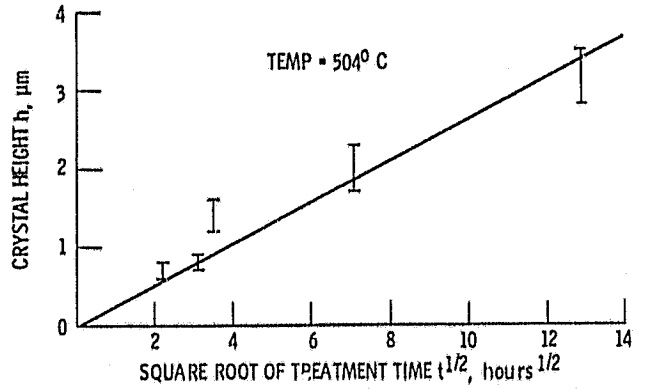

Figure 2. Maximum height of interfacial crystals as measured from scanning electron micrographs for isothermally-treated B/6061-A1 composites (ref. 2).

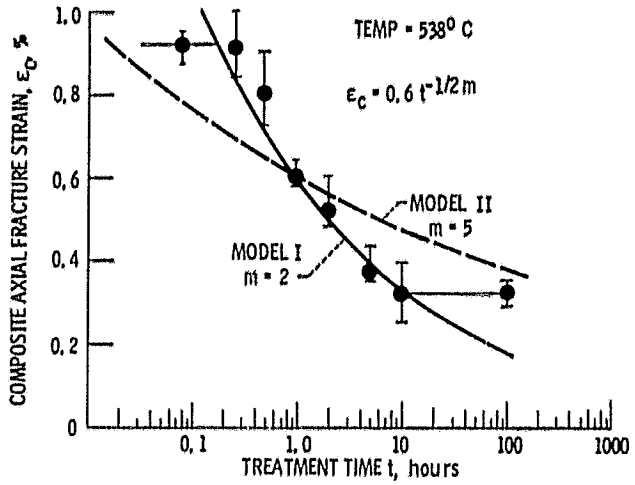

Figure 3. - Comparison of the time-dependent fracture strain predictions of models I and II with axial fracture strain data for isothermally-treated B/6061-Al composites (ref. 2).

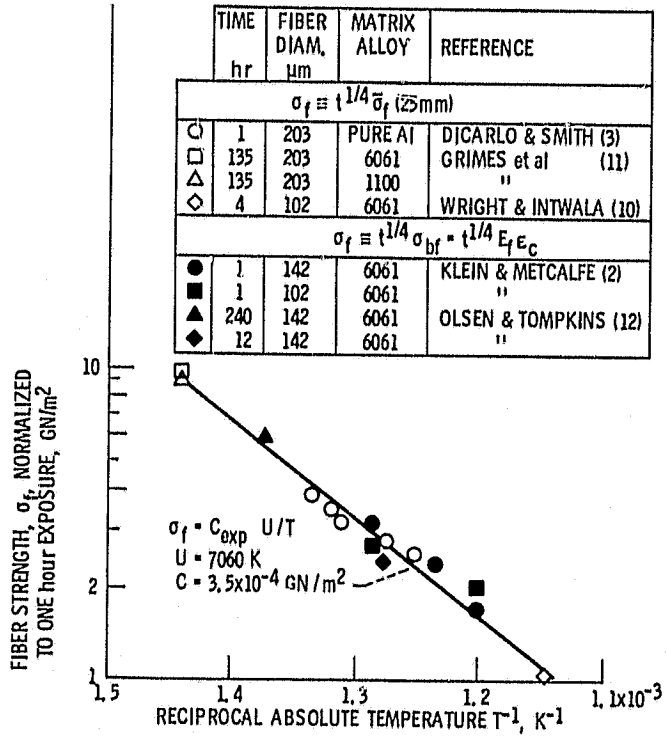

Figure 4. Comparison of fiber strength data with the time and temperature-dependent strength predictions of model I.

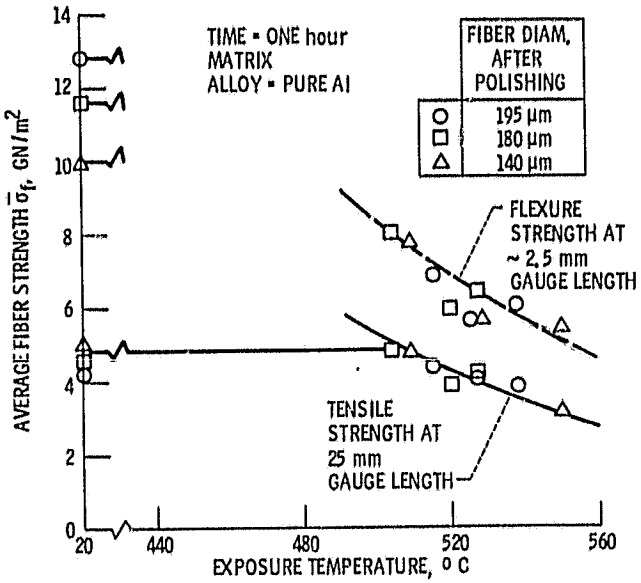

Figure 5. - Tensile and flexure strength degradation for heat-treated aluminum-coated boron fibers which were chemically polished prior to the coating and heat treatments (ref. 3).